PROCEEDINGS OF SCIENCE

Dedicated data analyses for improving PDFs: Study of proton parton distribution functions at high x and charm production in charged DIS at HERA

Ritu Aggarwal[*†]
On behalf of the ZEUS Collaboration
Savitribai Phule Pune University
E-mail: ritu.aggarwal1@gmail.com

Proton parton distribution functions (PDFs) are poorly constrained by existing data for Bjorken x larger than 0.6, and the PDFs extracted from global fits differ considerably from each other. A technique for comparing predictions based on different PDF sets to observed event numbers is presented. It is applied to compare predictions from the most commonly used PDFs to published ZEUS data at high Bjorken x. A wide variation is found in the ability of the PDFs to predict the observed results. A scheme for including the ZEUS high-x data in future PDF extractions is discussed.

Charm production in charged current deep inelastic scattering has been measured for the first time in $e^{\pm}p$ collisions, using data collected with the ZEUS detector at HERA, corresponding to an integrated luminosity of 358 pb^{-1} separately for $e^{+}p$ and $e^{-}p$ scattering at a centre-of-mass energy of $\sqrt{(}s)$ =318GeV within a kinematic phase-space region of 200 GeV2< Q^2 <60000 GeV2 and y <0.9, where Q^2 is the squared four-momentum transfer and y is the inelasticity. The measured cross sections of electroweak charm production are consistent with expectations from the Standard Model within the large statistical uncertainties.

40th International Conference on High Energy physics - ICHEP2020
July 28 - August 6, 2020
Prague, Czech Republic (virtual meeting)

[*]Supported by Dept. of Science and Tech. (DST), India.
[†]Speaker.

PoS(ICHEP2020)448

1. Introduction

This paper presents two of the latest ZEUS analyses that can prove to be very useful while unveiling the deep structure of proton at the kinematic region not known before. The ZEUS high-x analysis [1] provides the cross sections up to a Bjorken-x value of 1. The Neutral Current (NC) DIS HERA data already included in the Parton Distribution Function (PDF) extraction is up to a value of x of 0.65 [2]. Other than this, the PDF determination at the high-x region mostly rely on the data from the fixed target experiments [3, 4]. The high-x [1] data from HERA is the only Deep Inelastic Scattering (DIS) data reaching up to this high-x at high-Q^2. In the current new analysis from ZEUS [5] presented here on the high-x data, technique of building and using Transfer Matrix for the high-x data is demonstrated, which can be used by different PDFs to predict the number of events in the cross section bins.

In the second ZEUS analysis [6] presented here, an overview of making a measurement on the strange content of the proton through the charm production in Charged Current (CC) $e^{\pm}p$ DIS interactions at $\sqrt{s}$= 318 GeV is given. The measurement are done on the HERA-II data which fully explore the higher luminosities and improved heavy particle identification capabilities. The measured electroweak charm cross sections are found to be consistent with the Standard Model expectations.

2. Transfer Matrix Analysis at high-x

One of the reasons that high-x data [1] is not included in the PDF extraction is that some of the cross section bins expect and report very less number of events. These can not be included in a χ^2 fit PDF extraction directly. This problem becomes irrelevant when number of events expected from a PDF are compared to those reconstructed in the high-x cross-section bins using Poisson statistics. If $\lambda_{i,k}$ are the number of events generated in i^{th} true phase space bin using a given k^{th} PDF, then expectation of reconstructed events in any j^{th} bin, $\nu_{j,k}$ is given as

$$\nu_{j,k} = \sum_i T_{ij} R_{ii} \lambda_{i,k} \tag{2.1}$$

where R_{ii} are QED and QCD radiative corrections which result in migrations of events in the x-Q^2 phase space, and are calculated using HERACLES [7]. Here T_{ij} are the the Transfer Matrix elements; each element gives a probability that an event generated with i^{th} true x-Q^2 co-ordinates appears in the j^{th} cross section bin. It takes care of all detector effects including limited detector acceptance and various corrections applied on the simulated data [1].

The $\nu_{j,k}$, number of events expected in the j^{th} bin from k^{th} PDF can be compared to the number of events reconstructed in the data, n_j, and a probability P can be calculated as below

$$P(D|\mathrm{PDF_k}) = \prod_j \frac{e^{-\nu_{j,k}} \nu_{j,k}^{n_j}}{n_j!}. \tag{2.2}$$

Bayes factor can be calculated from the ratio of probabilities for different PDFs to predict the data, and an effective $\Delta\chi^2$ between two PDFs labelled as k and l is thus calculated using the equation given below

	e^-p			e^+p		
PDF	p-value	P1/P2	$\Delta\chi^2$	p-value	P1/P2	$\Delta\chi^2$
HERAPDF2.0	2.8×10^{-2}	1.0	0.0	0.35	1.0	0.0
CT14	3.2×10^{-3}	7.6×10^{-3}	9.8	0.82	$5.9\times10^{+5}$	-27
MMHT2014	2.3×10^{-3}	2.1×10^{-3}	12	0.82	$4.7\times10^{+5}$	-26
NNPDF3.1	3.9×10^{-4}	3.2×10^{-6}	25	0.73	$9.0\times10^{+4}$	-23
NNPDF2.3	1.3×10^{-4}	2.3×10^{-7}	31	0.70	$4.2\times10^{+4}$	-21
ABMP16	2.6×10^{-2}	9.0×10^{-1}	0.21	0.64	$6.1\times10^{+2}$	-13
ABM11	3.3×10^{-2}	7.2×10^{-1}	0.67	0.45	2.8	-2.1

Table 1: The p-values, Bayes Factors (P1/P2) and $\Delta\chi^2$ from comparisons of predictions using different NNLO PDF sets to the observed numbers of events. The Bayes Factor is calculated relative to HERAPDF2.0, as is $\Delta\chi^2$. The results are shown separately for the e^-p and e^+p data sets.

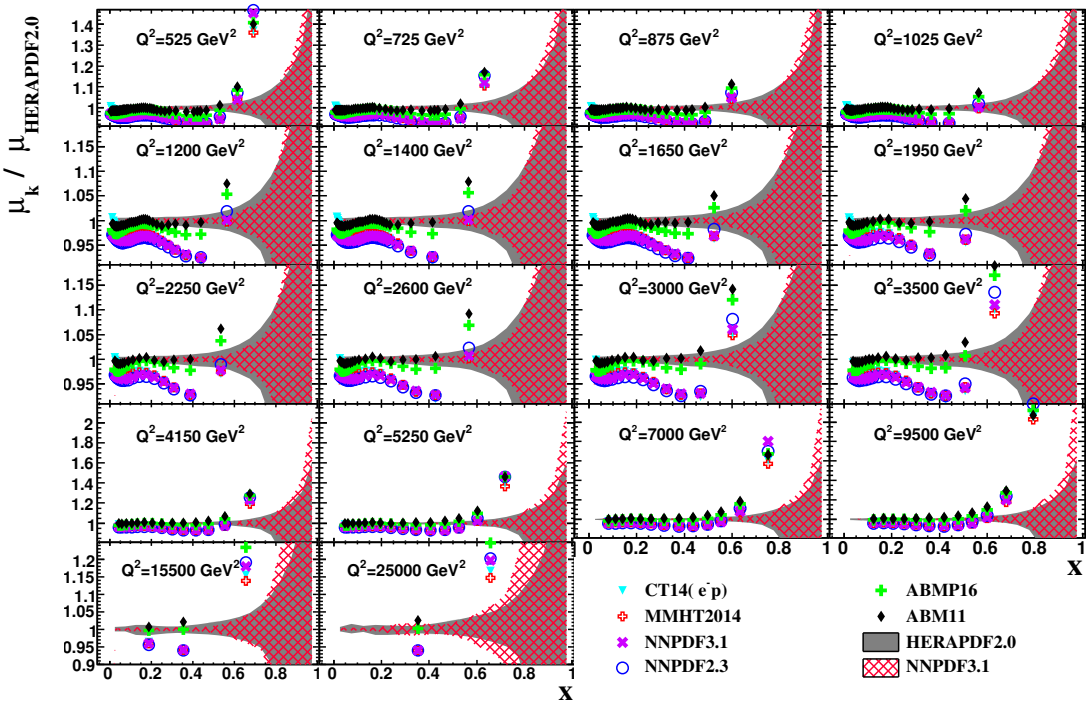

Figure 1: The ratio of the number of events generated using different PDFs to the expectations from the HERAPDF2.0 PDF set for e^-p data. The grey and red bands show PDF uncertainty calculated for the HERAPDF2.0 and NNPDF3.1 respectively on the expectation at the generator level.

$$\Delta\chi^2_{k,l} = -2\ln\frac{P(D|\mathrm{PDF}_k)}{P(D|\mathrm{PDF}_l)}\,. \tag{2.3}$$

The effective $\Delta\chi^2$ and p-values [8] give the goodness-of-fit of different PDF sets (CT14 [9], MMHT2014 [10], NNPDF3.1 [11], NNPDF2.3 [12], ABMP16 [13] and ABM11 [14]) and are shown in Table 1 for the e^-p and e^+p data samples. All the PDF sets are observed to give acceptable p-values showing an overall good agreement with the data. However, there are large differences amongst the PDFs themselves. The Bayes factor differ by 6 orders in magnitude which result in a corresponding $\Delta\chi^2$ of values up to 31.

The number of events generated using different PDFs, $\mu_{i,k} = R_{il} * \lambda_{i,k}$, are compared in the true x-Q^2 bins as shown in Figure 1 for the e^-p data set. It is observed that there are large differences in the numbers of events generated by different PDFs, and the differences cannot be explained by the PDF uncertainties. The large PDF uncertainties at very high-x and the differences between different PDFs further point towards the need of including the ZEUS high-x data in the PDF extraction.

3. ZEUS Charged Current charm Analysis

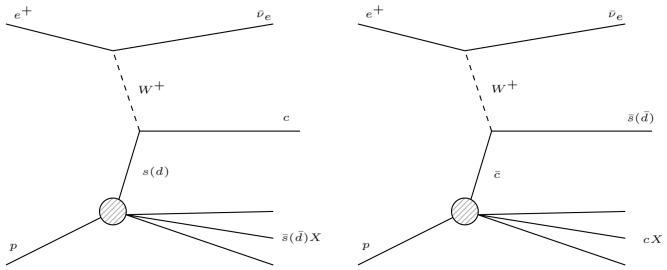

Figure 2: Feynmann diagram of charm-production sub processes via QPM interactions.

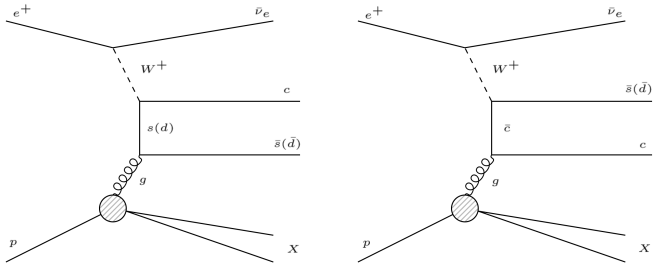

Figure 3: Feynmann diagram of charm-production sub processes via BGF interactions.

The motivation of the analysis is to probe the strange content of the proton via a CC interaction. The strange quark density distribution inside proton is a model dependent quantity and it's experimental values measured at the low-x regions are found to be inconsistent amongst different high energy experiments [15]-[18]. In a CC ep DIS interaction, a single charm quark in the final state can be produced at the level of Quark Parton Model (QPM) as shown in Figure 2 or via Boson Gluon Fusion (BGF) as shown in Figure 3. The electroweak process of interest is the one shown in

Figure 2 (left) where exchanged boson interacts with the strange sea quark, and the contribution of interaction via down or beauty quark are Cabibbo suppressed [19].

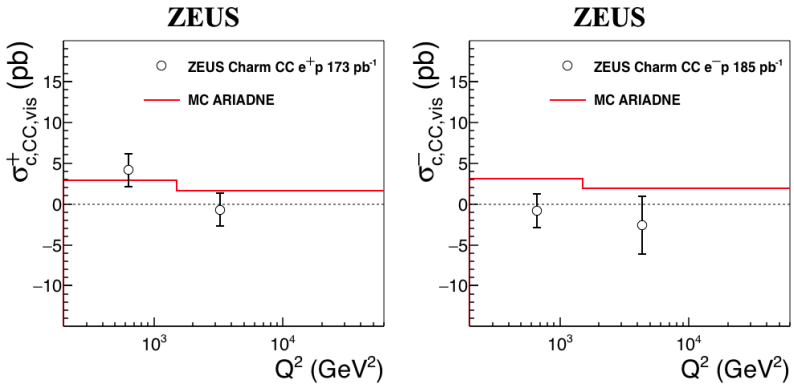

Figure 4: The visible charm cross sections in bins of Q^2 for e^+p and e^-p data samples.

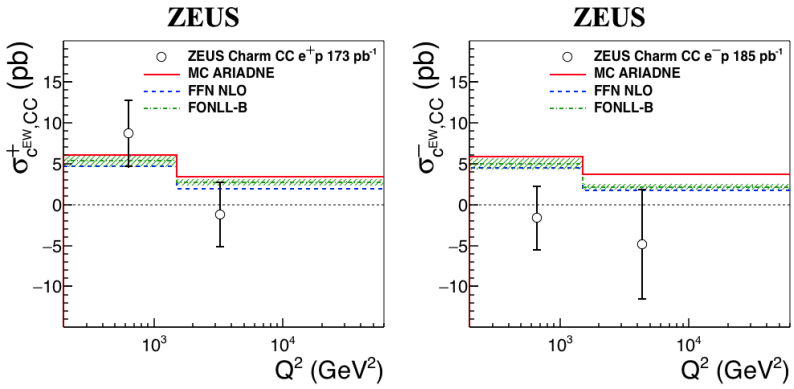

Figure 5: The total electroweak contribution to the visible charm cross sections in bins of Q^2 for e^+p and e^-p data samples.

The charged current DIS events have missing lepton information in the final state, because of which, Jacquet Blondel Method is used to reconstruct the kinematic variables which takes into account the final state hadronic information. The signal events with heavy quark in the final state are filtered in the data using the lifetime-tagging method. These events leave a signature in the detector in the form of secondary-vertex as they travel a measurable distance before decaying, whereas the light flavor will decay promptly. The transverse decay length of the secondary vertices will be symmetric with respect to the primary vertex (due to the limited resolution of the detector), whereas for the heavy quark it will be asymmetric. The light flavor background can be eliminated by subtracting negative decay length distribution from the positive decay length.

The EW contribution ($\sigma_{c^{EW},vis}$) in the total visible charm cross section ($\sigma_{c,vis}$) should be obtained by subtracting from it the BGF contribution (Figure 3). However, due to imprecise and small predictions by Ariadne 4.12, this contribution is not subtracted and is included as a systematic uncertainty. The total visible charm cross section is extrapolated using a factor C_{ext} to obtain the EW contribution. Factor C_{ext} is calculated as a ratio of number of charm events generated in the full kinematic region (N^{EW}_{gen}) to the number of charm events of EW origin in the visible kinematic region (N^{EW}_{vis}). The EW charm cross section is given as

$$\sigma_{c^{EW}} = C_{ext}\,\sigma_{c,vis}. \tag{3.1}$$

The total charm cross section and the resulting total EW charm cross sections for the e^+p and e^-p data samples are shown in Figure 4 and Figure 5 respectively.

4. Discussion

The ZEUS high-x data has shown a great discriminating power in the high-x region. Different PDFs show large differences amongst themselves in terms of p-values and $\Delta\chi^2$ when compared to the high-x data. Despite the fact that the event numbers in ZEUS high-x data are small, this data set contains significant information on the behavior of the parton densities. Transfer Matrix has been built for the ZEUS high-x data and the technique to use it to predict number of events in the cross section bins from different PDFs is shown.

The ZEUS charm cross sections in the Charged current DIS interactions are presented. This data covers a wide range in Q^2 and is sensitive to the strange sea content of the proton. This data will complement the recent results from different high energy physics experiments in probing the strange sea density inside the proton.

References

[1] ZEUS Coll., H. Abramowicz et al., Phys. Rev. **D 89**, 072007 (2014).

[2] ZEUS Coll., H. Abramowicz et al., Eur. Phys. **J. C 75**, 580 (2015).

[3] BCDMS Coll., A.C. Benvenuti et al., Phys. Lett. **B 223**, 485 (1989).

[4] L.W. Whitlow et al., Phys. Lett. **B 282**, 475 (1992).

[5] ZEUS Coll., I. Abt et al., Phys. Rev. **D 101**, 112009 (2020).

[6] ZEUS Coll., I. Abt et al., JHEP **05**, 201 (2019).

[7] A. Kwiatkowski, H. Spiesberger and H.-J. Möhring, Comp. Phys. Comm. **69**, 155 (1992). Also in *Proc. Workshop Physics at HERA*. eds. W. Buchmüller and G. Ingelman, (DESY, Hamburg, 1991).

[8] F. Beaujean et al., Phys. Rev. **D 83**, 012004 (2011).

[9] S. Dulat et. al., Phys. Rev. **D 93**, 033006 (2016).

[10] L. Harland-Lang, A. D. Martin, P. Motylinski, and R. Thorne, Eur. Phys. J. **C 75**, 204 (2015).

[11] R. D. Ball et al., Eur. Phys. J. **C 77**, 663 (2017).

[12] R. D. Ball et al., Nucl. Phys. **B 867**, 244 (2013).

[13] S. Alekhin, J. Blümlein, S. Moch, and R. Placakyte, Phys. Rev. **D 96**, 014011 (2017).

[14] S. Alekhin, J. Blümlein, and S. Moch, Phys. Rev. **D 86**, 054009 (2012).

[15] NuTeV Collaboration, Phys. Rev. **D 64**, 112006 (2001).

[16] NOMAD collaboration,Nucl. Phys. **B 876**, 339 (2013).

[17] ATLAS collaboration,Eur. Phys. J. **C 77**, 367 (2017).

[18] CMS collaboration, JHEP **02**, 013 (2014). CMS collaboration, Eur. Phys. J. **C 79**, 269 (2019).

[19] Abramowicz and Caldwell, Rev. Mod. Phys. **71**, 1275-1410 (1999).

PoS(ICHEP2020)448